

Computational Studies of Physical Properties of Nb-Si Based Alloys

DOE Grant # DE-FE-0003798

Lizhi Ouyang (PI)
Tennessee State University

Pittsburgh, PA
May 30, 2012

- ❑ Develop a software package to facilitate the first principles calculations of physical properties of crystals and solid solutions commonly found in alloys.

- ❑ Compute thermodynamic and mechanical properties of various phases found in the Nb-Si-Cr-X alloy systems.

- First principles calculations based on DFT (VASP)
- Born-Oppenheimer approximation
- Harmonic model for vibrational free energy
- Quasi-harmonic approximation for first order anharmonicity
- Berry phase approach for polarization
- RPA for optical properties

- Helmholtz free energy $F(\{\mathbf{a}\}, T)$

$$F(\{\mathbf{a}\}, T) \approx E^c(\{\mathbf{a}\}) + F^{el}(\{\mathbf{a}\}, T) + F^v(\{\mathbf{a}\}, T)$$

- Electron excitation free energy:

- Mermin's finite temperature DFT:
- Non-interacting reference frame

$$F = \underset{n(r,T)}{\text{Min}}\{E - TS\}$$

$$F^{el}(\{\mathbf{a}\}, T) \approx \sum_i \left\{ (\epsilon_F - \epsilon_i) - k_B T \ln \left(1 + e^{(\epsilon_F - \epsilon_i)/k_B T} \right) \right\}$$

- Vibrational free energy:

- Quantum harmonic oscillators: (non-interacting phonon model)
- *Anharmonic effect through phonon perturbation theory*

$$F^v(\{\mathbf{a}\}, T) \approx \sum_i \left\{ \frac{1}{2} \hbar \omega_i - k_B T \ln \left(1 - e^{-\hbar \omega_i / k_B T} \right) \right\}$$

- Potential energy due to external fields:

- *electric field, magnetic field*

- **Harmonic Model:** non-interacting reference frame

$$\mathbf{H} = \frac{1}{2} \sum_i \left\{ p_i^2 + \omega_i^2 q_i^2 \right\}$$

- **Quasi-Harmonic Approximation**

$$\omega_i(\{\mathbf{a}\}, T) \approx \omega_i(\{\mathbf{a}\})$$

- **Dynamical matrix**

➤ *finite difference approximation*

$$D_{\mu\nu} \left(\begin{matrix} \bar{q} \\ k k' \end{matrix} \right) = \frac{1}{\sqrt{m_k m_{k'}}} \sum_l \Phi_{0k_\mu, lk'_\nu} e^{i \bar{q} \cdot (u_{l k'} - u_{0k})}$$

$$\Phi_{lk_\mu, l'k'_\nu} = -\frac{\partial F_{lk_\mu}}{\partial u_{l'k'_\nu}} \approx -\frac{\Delta F_{lk_\mu}}{\Delta u_{l'k'_\nu}}; \quad \Phi_{lk, l'k'} = 0 \quad \text{for} \quad |r_{lk} - r_{l'k'}| > R_{\text{cutoff}}$$

- **LO/TO splitting**

- *Born effective charge calculated using Berry phase method*
- *LO/TO splitting calculated using Born effective charge*

Supercell finite difference approach:

$$\Phi_{lk, l'k'} = 0 \quad \text{for} \quad |r_{lk} - r_{l'k'}| > R_{\text{cutoff}}$$

Density functional perturbations theory:

$$D_{\mu\nu} \left(\begin{matrix} q \\ k k' \end{matrix} \right) = \frac{1}{\sqrt{m_\mu m_\nu}} \frac{\partial^2 E}{\partial u_{\mu k}^q \partial u_{\nu k'}^q}$$

□ Physical properties

- *Energies: $F(\{a\}, T)$, $U(\{a\}, T)$*
- *1st order derivatives: $\sigma(\{a\}, T)$, $S(\{a\}, T)$*
- *2nd order derivatives: $C_V(\{a\}, T)$, $C(\{a\}, T)$, $\alpha(\{a\}, T)$, $\gamma(\{a\}, T)$*
- *Higher order derivatives ...*

□ Free energy of imperfect crystal

G(P,T) Module: Structure modeling

gensurf: automated surface slab model generation

genbyteplate: automated structural model generation based on structure template: (For example, *Strukturbericht* symbols **A8**)

gensolsol: automated supercell structural model generation for crystals with partial occupations

General case:

$$C_{ij}(\{\mathbf{a}\}, T) = \frac{\partial^2 F(\{\mathbf{a}\}, T)}{\partial \boldsymbol{\varepsilon}_i \partial \boldsymbol{\varepsilon}_j}$$

Challenges:

- *seven parameters: $\{\mathbf{a}\}, T$*
- *instability zone*

Hydrostatic case:

$$C_{ij}(P, T) = \frac{\partial^2 F(\{\mathbf{a}\}, T)}{\partial \boldsymbol{\varepsilon}_i \partial \boldsymbol{\varepsilon}_j} \bigg|_{\frac{\partial F(\{\mathbf{a}\}, T)}{\partial \boldsymbol{\varepsilon}_i} = -P \lambda_i} \quad \text{where } \lambda_i = \begin{cases} 1, & i = 1, 2, 3 \\ 0, & i = 4, 5, 6 \end{cases}$$

For small finite strain on a periodic structure $\{\mathbf{a}\}$

$$F(\{a\}, T) = F(\{a\}_0, T) - V_0 \sum_i \sigma_i(\{a\}_0, T) \varepsilon_i + \frac{1}{2} V_0 \sum_{ij} C_{ij}(\{a\}_0, T) \varepsilon_i \varepsilon_j + O[\varepsilon^3]$$

$$S(\{a\}, T) = S(\{a\}_0, T) + V_0 \sum_i \frac{\partial \sigma_i(\{a\}_0, T)}{\partial T} \varepsilon_i - \frac{1}{2} V_0 \sum_{ij} \frac{\partial C_{ij}(\{a\}_0, T)}{\partial T} \varepsilon_i \varepsilon_j + O[\varepsilon^3]$$

$$C_V(\{a\}, T) = C_V(\{a\}_0, T) + V_0 T \sum_i \frac{\partial^2 \sigma_i(\{a\}_0, T)}{\partial T^2} \varepsilon_i - \frac{1}{2} V_0 T \sum_{ij} \frac{\partial^2 C_{ij}(\{a\}_0, T)}{\partial T^2} \varepsilon_i \varepsilon_j + O[\varepsilon^3]$$

For a local quadratic energy expansion:

$$\text{if } \{a\}_{P,T} \sim \{a\}_0$$

$$\rightarrow V_0 C_{ij}(\{a\}_0, T) \approx V(P, T) C_{ij}(\{a\}_{P,T}, T)$$

where

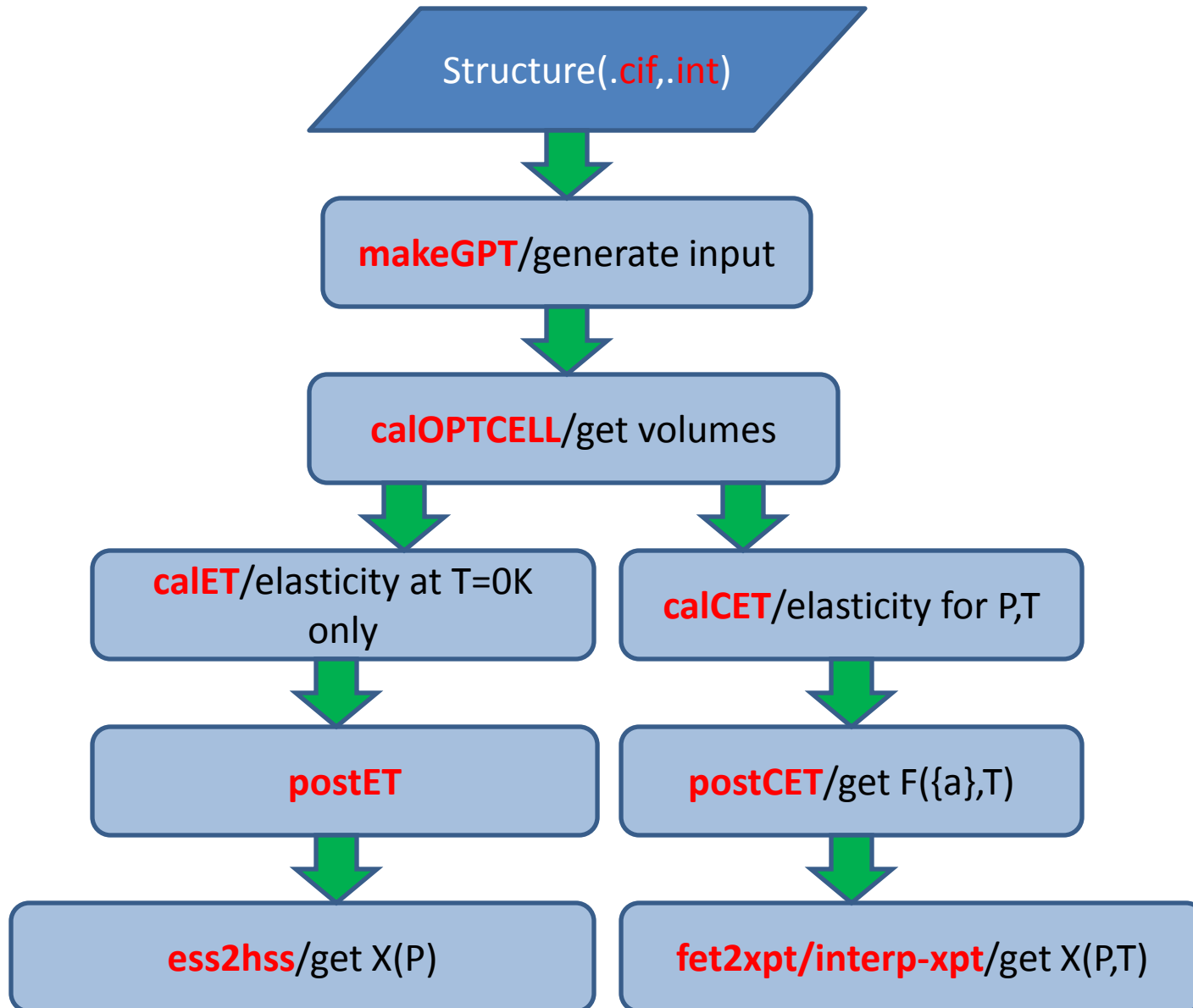
$$\{a\}_{P,T} = \{a\}_0 (I + \boldsymbol{\varepsilon}(P, T))$$

$$\boldsymbol{\varepsilon}_i(P, T) = \sum_j S_{ij}(\{a\}_0, T) (P \lambda_j - \sigma_j(\{a\}_0, T))$$

For each sampling volume V_k falls within the targeted P and T range:

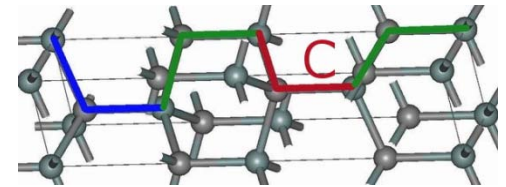
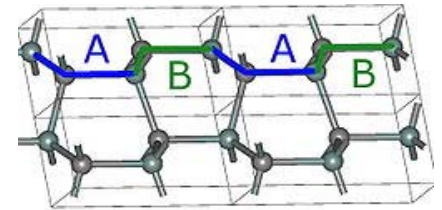
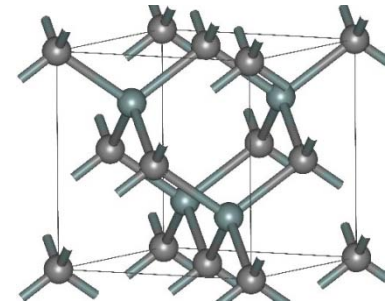
1. Geometry optimization at $T=0K$ to obtain $\{a\}_0^k$:
2. Applied a set of small strains $\{\epsilon^i\}$ to $\{a\}_0^k$: ($\{a\}_i^k$)
symmetry constrains applied to reduce # of strains
3. Calculate Helmholtz free energy for strained structure $\{a\}_i^k$:
4. **Symmetry constrained fitting** of $F(\{a\}_i^k, T)$, $S(\{a\}_i^k, T)$ and $C_V(\{a\}_i^k, T)$ of strained structures against the isothermal quadratic model to obtain:
elastic constants and their temperature derivatives (2nd order)
stress and its temperature derivatives (1st order)

* *For systems with large anisotropy, larger strains will be needed.*



Example: Silicon Carbide

- Very important material
 - high hardness
 - high sublimation temperature
 - high chemical inertness
 - high thermal conductivity
 - high electric field breakdown strength
 - high maximum current density
 - low thermal expansion/no discontinuity
 - ...



❑ VASP parameters:

- PAW GGA-PBE pseudopotential
- energy cutoff 500eV
- energy convergence 1.0E-8eV/cell
- force convergence -1.0E-4 eV/Å
- 3x3x3 supercell for 3C-SiC and 3x3x2 supercell for 2H-SiC
- K-points 5x5x5 for 3C-SiC and 5x5x4 for 2H-SiC [supercell]

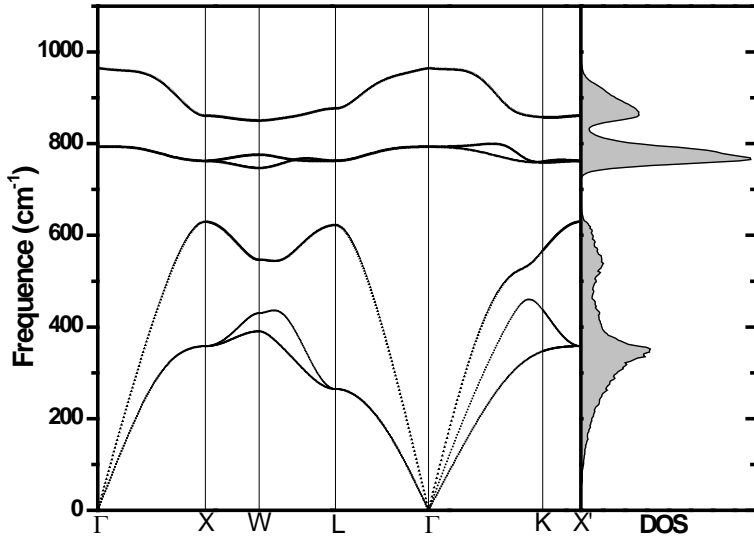
❑ Pressure [0-20GPa] and temperature [0-2500K]

❑ LO/TO splitting included in phonon calculations

❑ Properties:

- free energy, entropy, specific heat, thermal expansion
- elastic constants

3C-SiC



2H-SiC

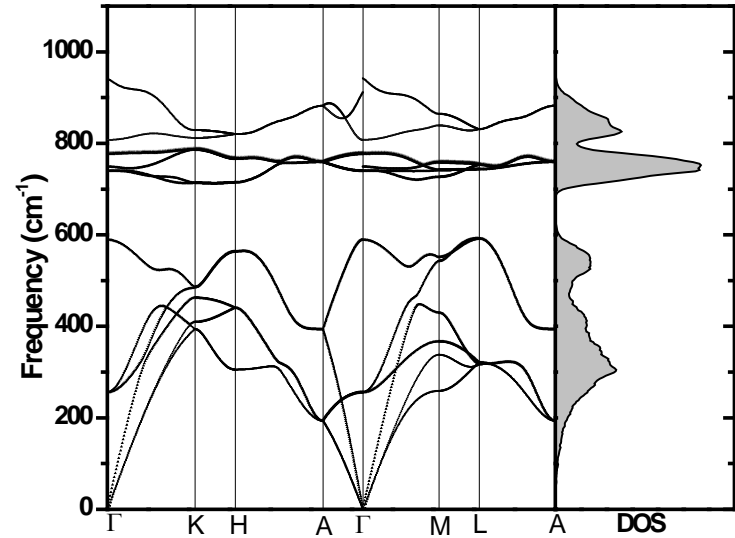
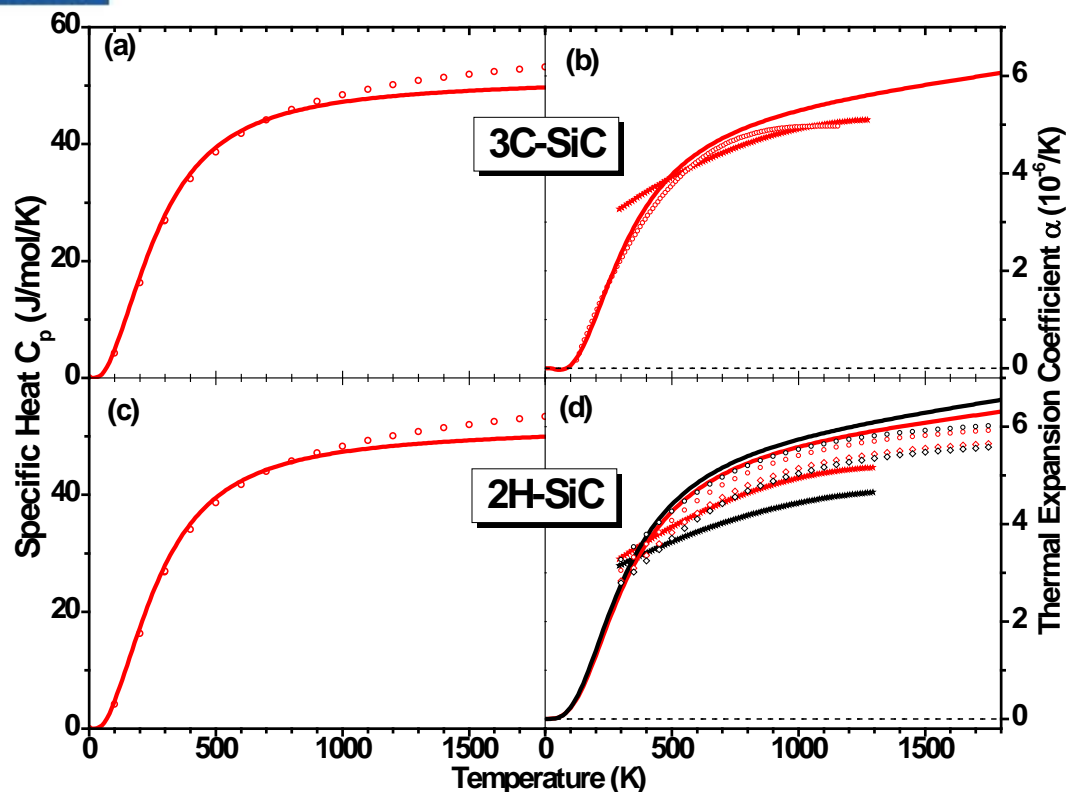


Table I. Zone-centered vibrational modes.

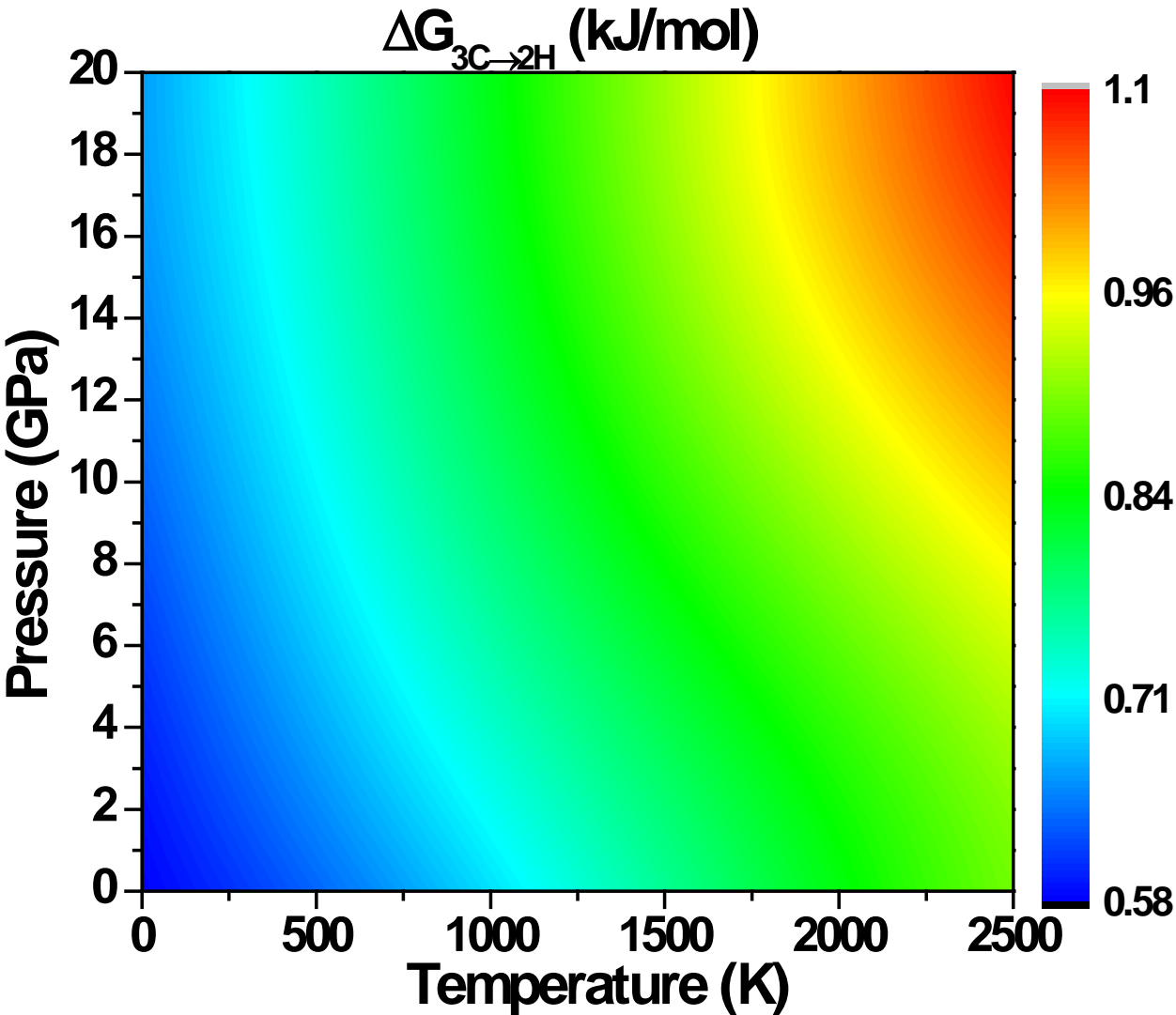
Branch	$\lambda(\text{cm}^{-1})$	Branch	$\lambda(\text{cm}^{-1})$
2H-SiC		3C-SiC	
E2	256.3	TO	793.5(796.2 ^a)
B1	589.2	LO	964.2(972.2 ^a)
E2	740.0		
A1	749.2		
E1(TO/LO)	777.4/941.6		
B1	807.2		

a) Experimental data from Ref.⁹

Specific heat and thermal expansion



Thermodynamic properties at $P=0$ up to 1800 K. Solid lines represent the calculated results. (a) Specific heat C_p of 3C. Empty circles are plotted using the experimental data. (b) Thermal expansion coefficient of 3C. Empty circles and solid stars are experimental values respectively. (c) Specific heat C_p of 2H. Empty circles are the experimental data from Ref. 10 (d) Thermal expansion coefficient of 2H. The red symbols are α_{11} and the black symbols are α_{33} . The circles and diamonds are recent data from Ref. 14 for undoped single crystals of 6H-SiC and 4H-SiC, respectively. The solid stars are from Ref. 13

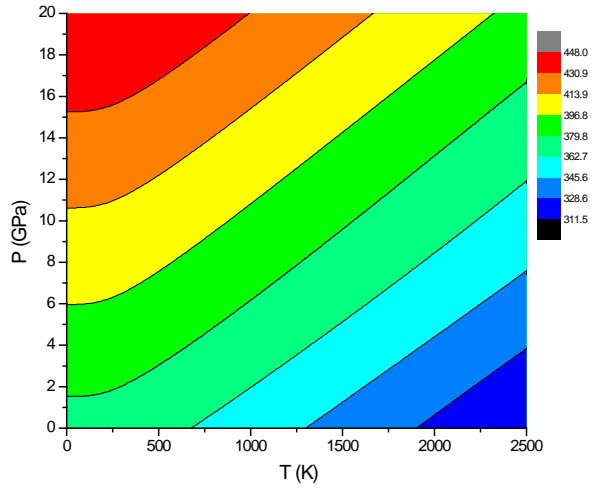


Contour plot of the Gibbs free energy difference from 3C-SiC to 2H-SiC.

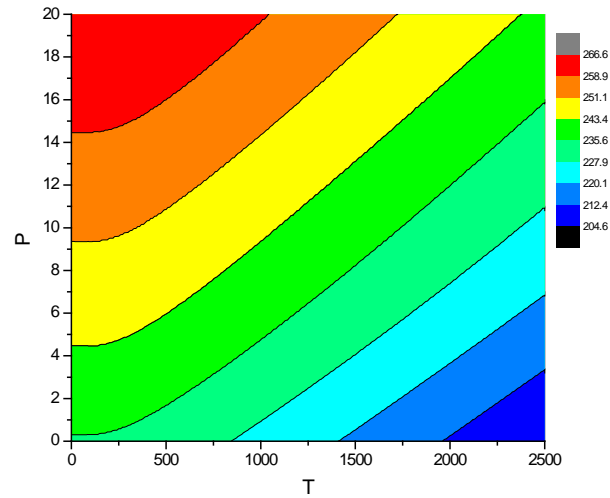
Observations:

- 3C is more stable at all plotted temperature pressure range
- Difference is smaller than commonly accepted DFT accuracy
- Increasing trend of free energy difference at higher pressure and temperature indicates that the experimental observed high temperature stability of 2H is likely due to defects/impurity not included in present calculations

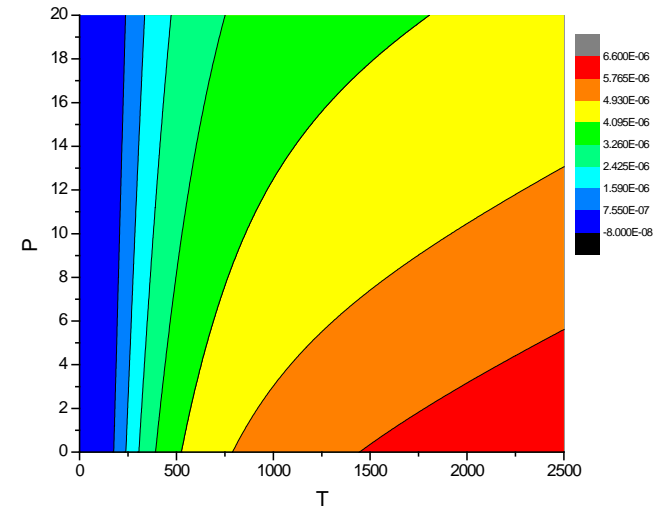
Elastic constants



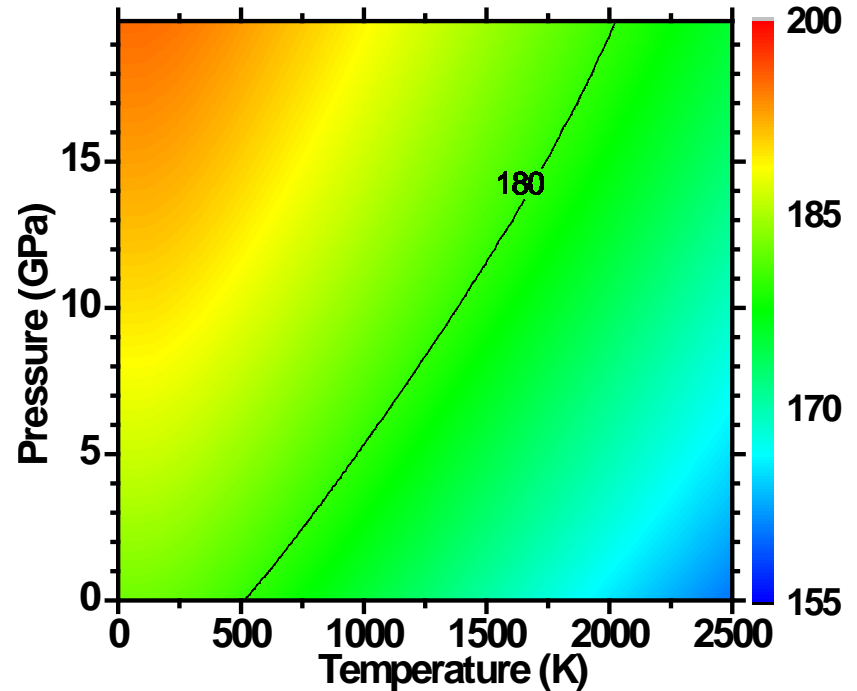
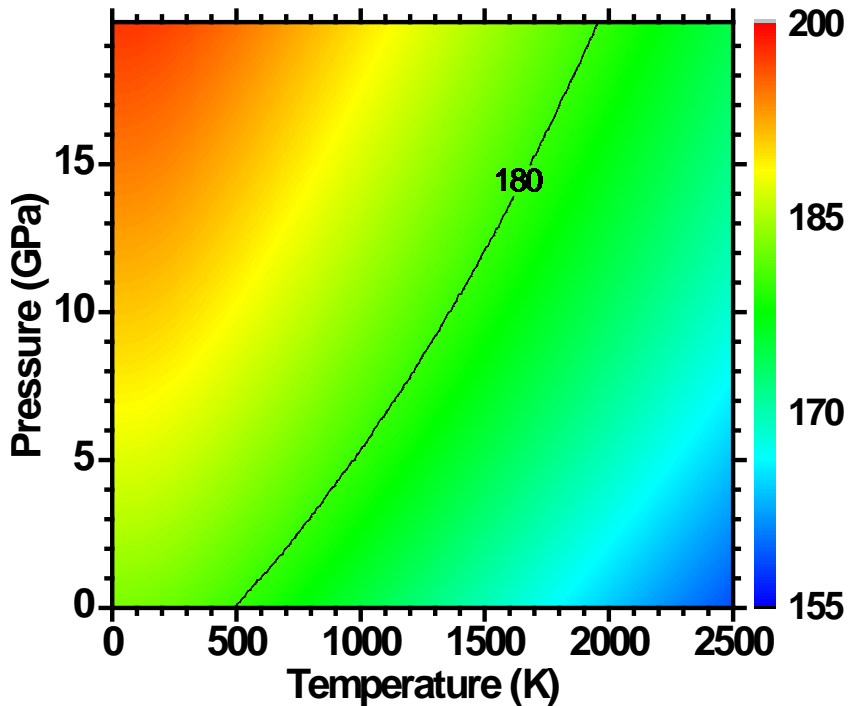
$C_{11}(P,T)$ -3C-SiC



$C_{44}(P,T)$ -3C-SiC



$\alpha(P,T)$ -3C-SiC



Contour plots of shear modulus for (a) 3C-SiC and (b) 2H-SiC.

The difference is very small. Shear modulus at high temperature and high pressure region is almost the same as that at ambient condition.

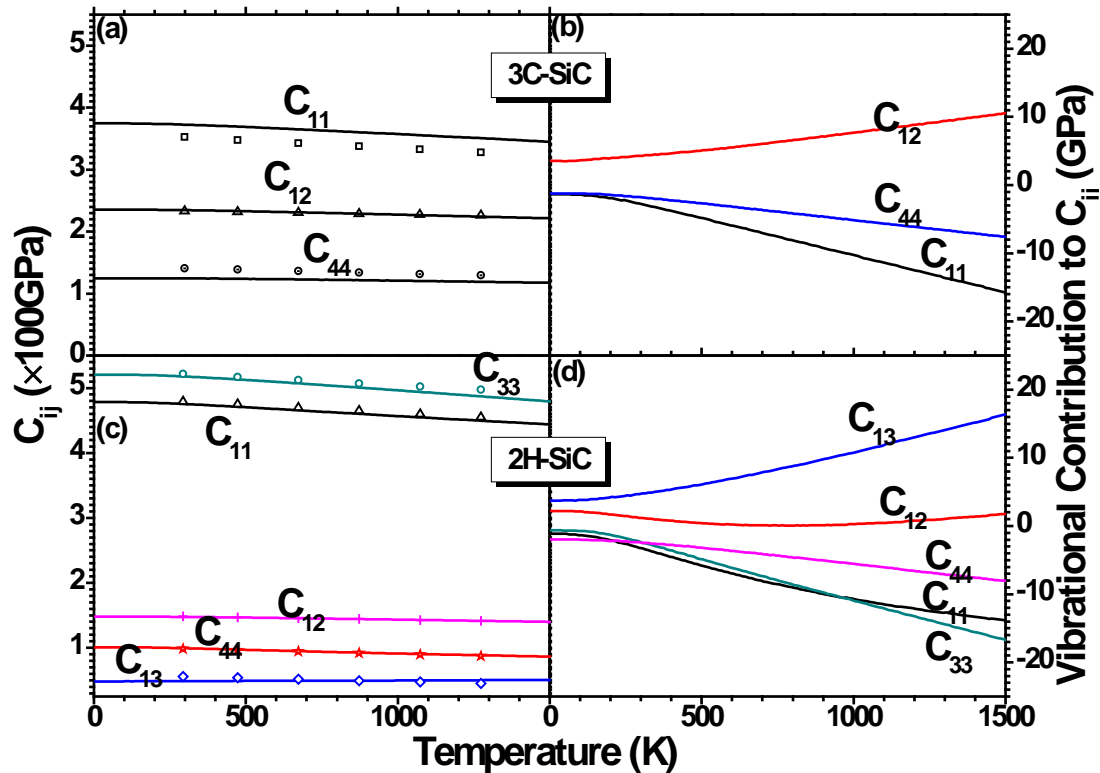
Under ambient pressure,

$$G_{2\text{H-SiC}} (T=298\text{K}) = 181 \text{ GPa}$$

$$G_{2\text{H-SiC}} (T=1773\text{K}) = 166 \text{ GPa}$$

$$\text{Experiment } 179 \pm 5 \text{ GPa}$$

$$\text{Experiment } 165 \pm 5 \text{ GPa}$$

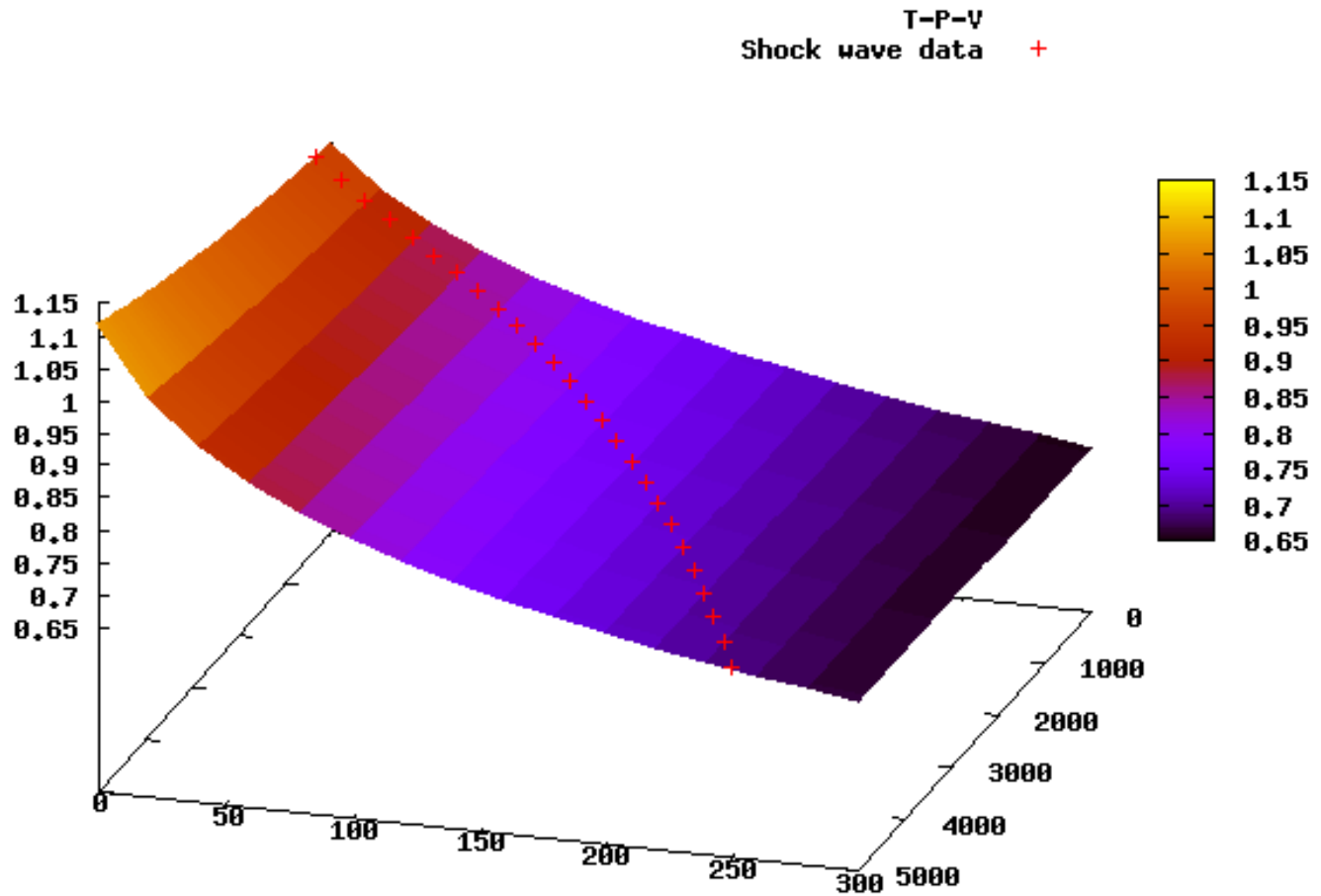


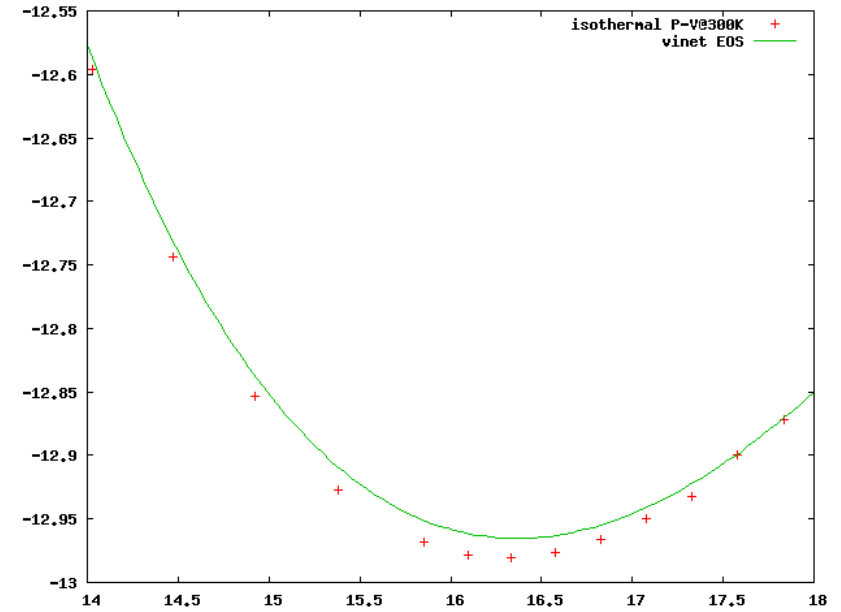
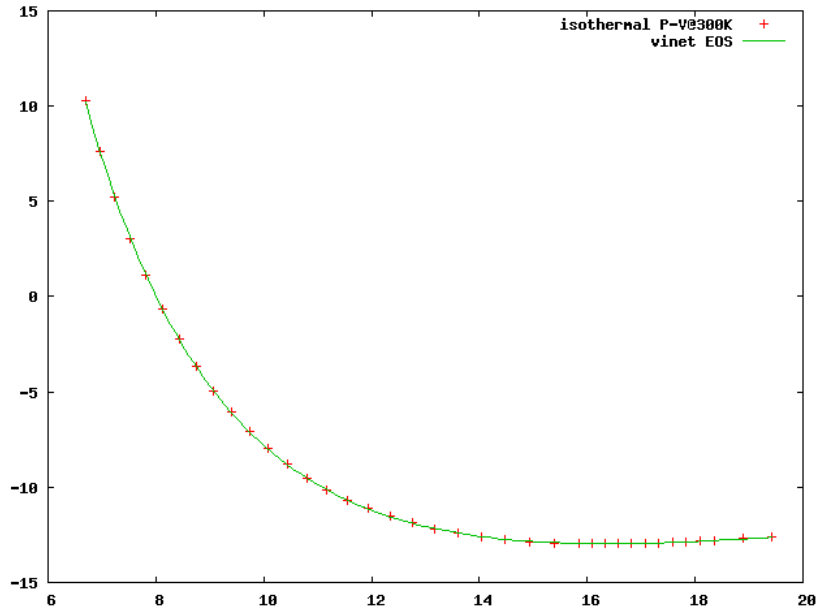
Temperature-dependent elastic constants at ambient pressure. Solid lines are the calculated properties and the symbols are from experimental measurements. (a) and (b) plot the elastic constants and thermal excitation contribution to elastic constants of 3C-SiC. (c) and (d) show the elastic constants and thermal excitation contribution to elastic constants of 2H-SiC.

G(P,T) Module: Equation of State (P-V-T)

- ❑ Helmholtz free energy $F(V,T)$ calculated from the G(P,T) package
- ❑ Compute pressure $P(V,T) = -\partial F(V,T) / \partial V$

- ❑ BCC alpha phase
- ❑ VASP setting:
 - PAW-GGA-PBE pseudopotential
 - energy convergence $1.0\text{E-}8\text{eV/cell}$
 - force convergence $-1.0\text{E-}4\text{ eV/\AA}$
 - 3x3x3 supercell
- ❑ Pressure range [0-1000GPa] and Temperature [0-5000K]
- ❑ Equation of states calculations (P-V-T)





Vinet EOS insufficient to fit the E-V data for pressure up to 1500GPa

Cluster Expansion Method for multi-component systems:

$$E(\vec{\sigma}) = \sum_{\alpha,s} m_{\alpha} J_{\alpha}^s \Phi_{\alpha}^s$$

Challenges: number of clusters grows rapidly

- (1) number of disordered sublattices $\sim (N_{\text{sublattice}})^{|\alpha|}$
- (2) number of components $\sim (N_{\text{component}} - 1)^{|\alpha|}$

Unitcell Expansion Method: *type of unitcell* \sim component

$$E(\vec{\eta}) = \sum_{\beta,s} m_{\beta} J_{\beta}^s \Phi_{\beta}^s$$

Rationale: 1-sublattice and increased number of components

- (1) Conceptually simple and easy to program
- (2) Smaller cluster $|\beta|$ needed (*possibly only pairs*)
- (3) Only a small set of unitcells may be needed

Cluster Expansion Method for multi-component systems:

$$E(\vec{\sigma}) = \sum_{\alpha,s} m_{\alpha} J_{\alpha}^s \Phi_{\alpha}^s$$

Challenges: number of clusters grows rapidly

- (1) number of disordered sublattices $\sim (N_{\text{sublattice}})^{|\alpha|}$
- (2) number of components $\sim (N_{\text{component}} - 1)^{|\alpha|}$

Unitcell Expansion Method: *type of unitcell* \sim component

$$E(\vec{\eta}) = \sum_{\beta,s} m_{\beta} J_{\beta}^s \Phi_{\beta}^s$$

Rationale: 1-sublattice and increased number of components

- (1) Conceptually simple and easy to program
- (2) Smaller cluster $|\beta|$ needed (*possibly only pairs*)
- (3) Only a small set of unitcells may be needed

First Principle calculations on small supercells built from selected unitcells

Solve the over determined equations to find out the effective cluster interactions (ECI)

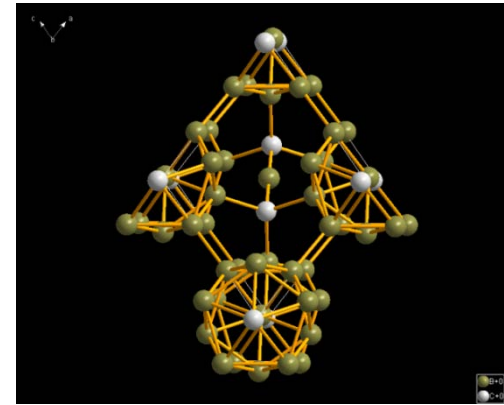
Monte Carlo simulations to calculate the free energy of $B_{4+x}C_{1-x}$ crystals

The large supercell's energy is calculated by ECI instead of first principle calculation

Challenges:

- (1) partial occupation possible at all 15 sublattices
- (2) highly correlated local structure B₁₂ icosahedron

Computationally prohibitive to do with traditional cluster expansion method as cluster size up to 12 may be needed



Unitcell Expansion:

Energy of the disordered model is expressed in clusters of unitcells.

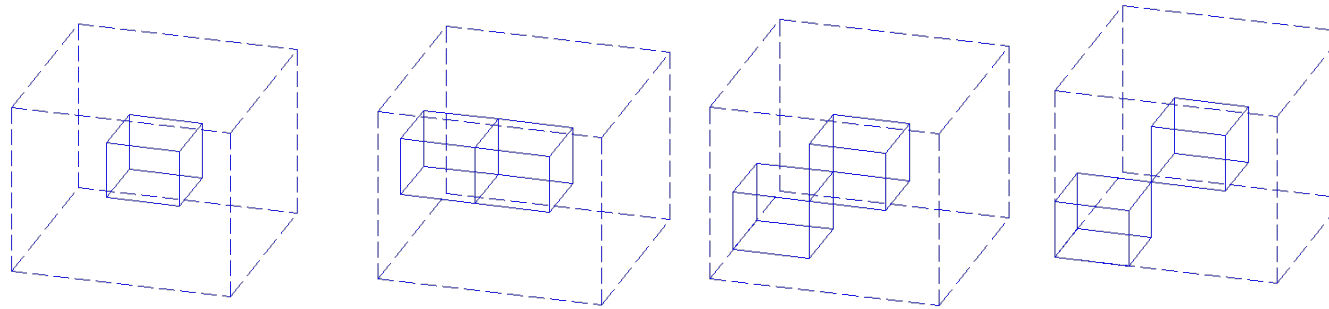
$$E(\vec{\eta}) = \sum_{\beta \subset \{\eta_i\}} m_{\beta} J_{\beta} \prod_{p \in \beta} \eta_p$$

In practice, we only expand the energy up to pair of unitcells since the unitcell is already fairly large.

Proper selection of unitcells is critical here: there are total 2^{15} models possible for all concentrations.

Clusters:

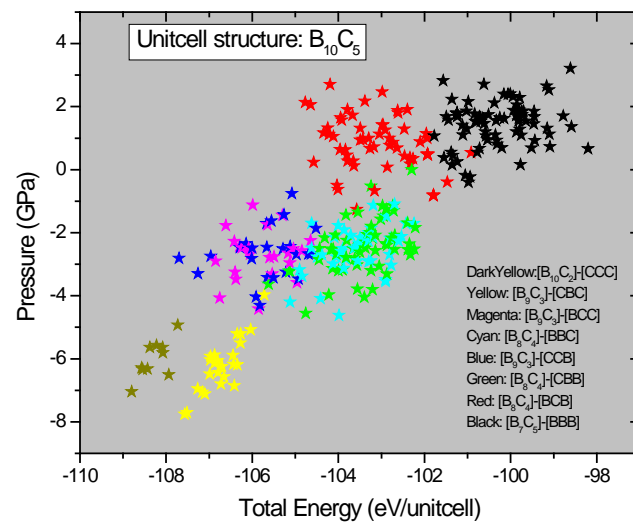
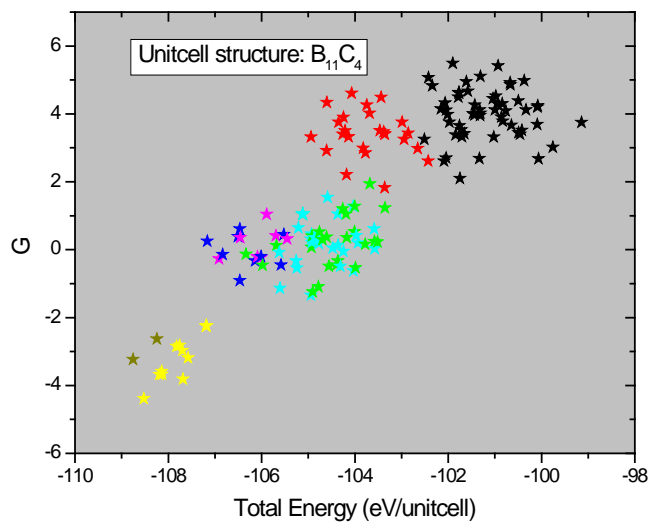
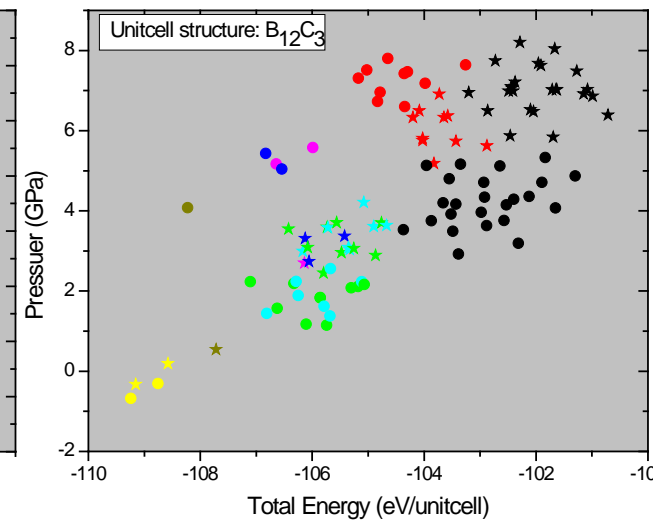
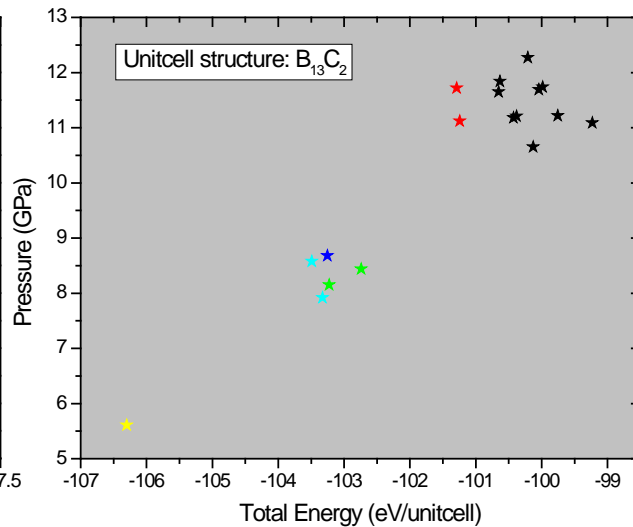
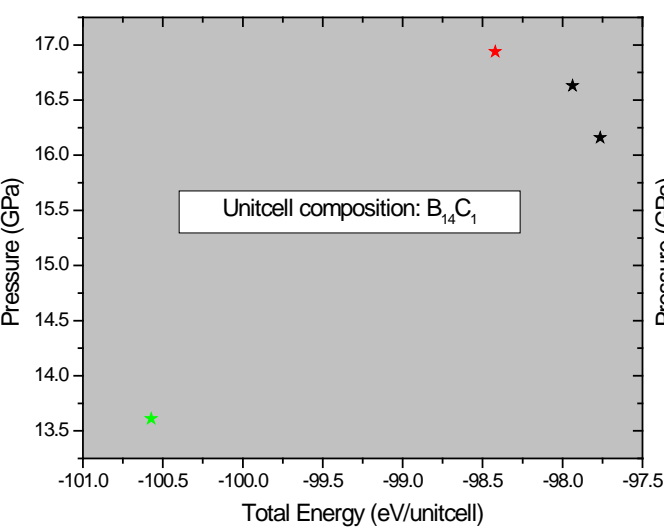
- (1) self
- (2) face-share
- (3) edge-share
- (4) corner-share



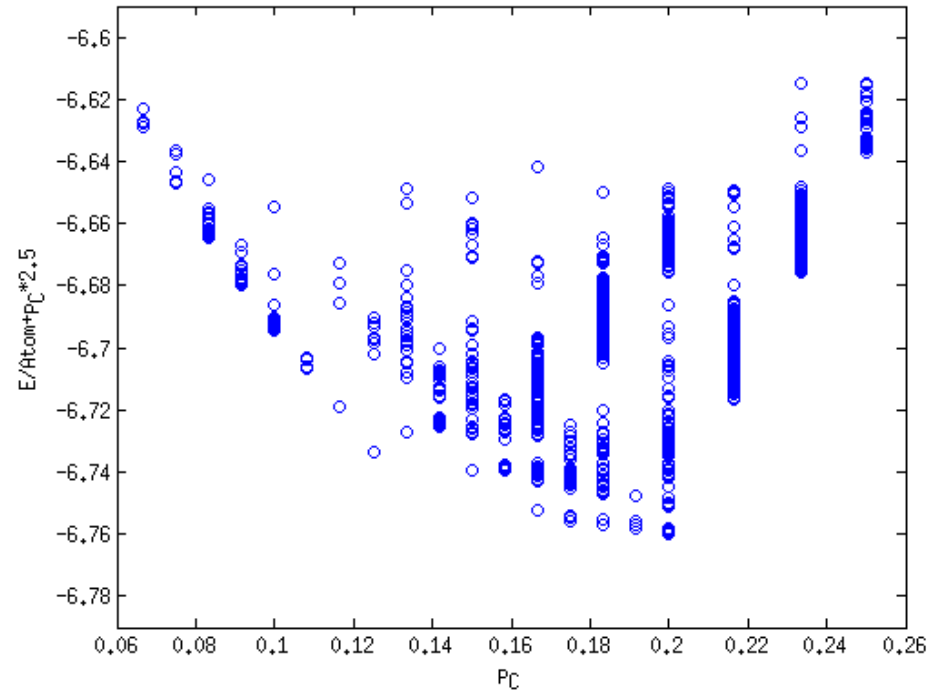
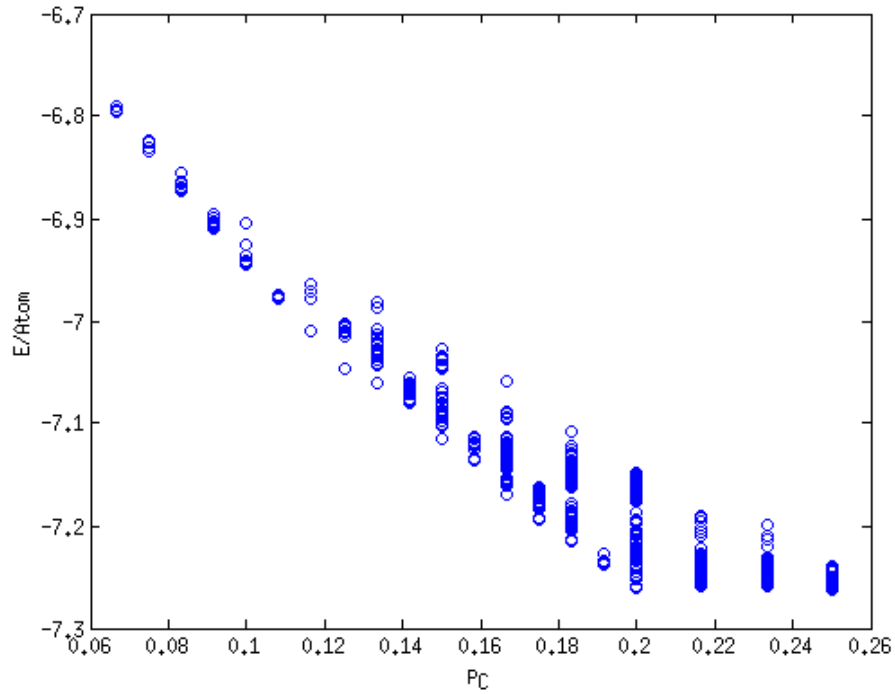
Unitcell Selection:

- (1) for periodic structures consisted of one type of unitcell
compute the total energy and pressure
- (2) group analysis of the total energies and pressures of the unitcells with the same concentration
- (3) select the lowest group in the total energies-pressure plot to be included in the set of unitcells (prefers unitcells with minimal intercell interactions)
- (4) it is possible to add more unitcells to the set using the criteria of cross-validation

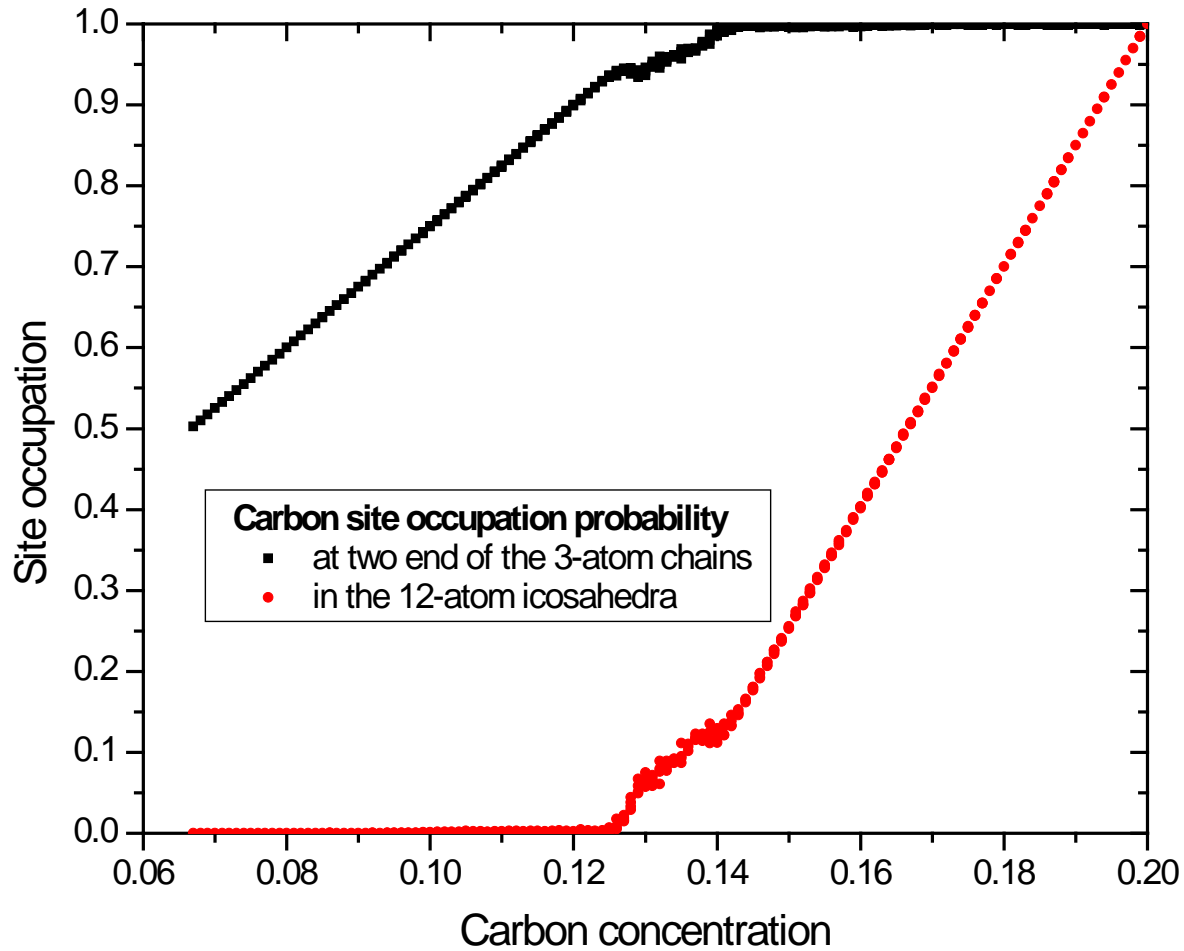
Concentration dependent periodic unitcell energies



Convex Plot of Supercell Sampling

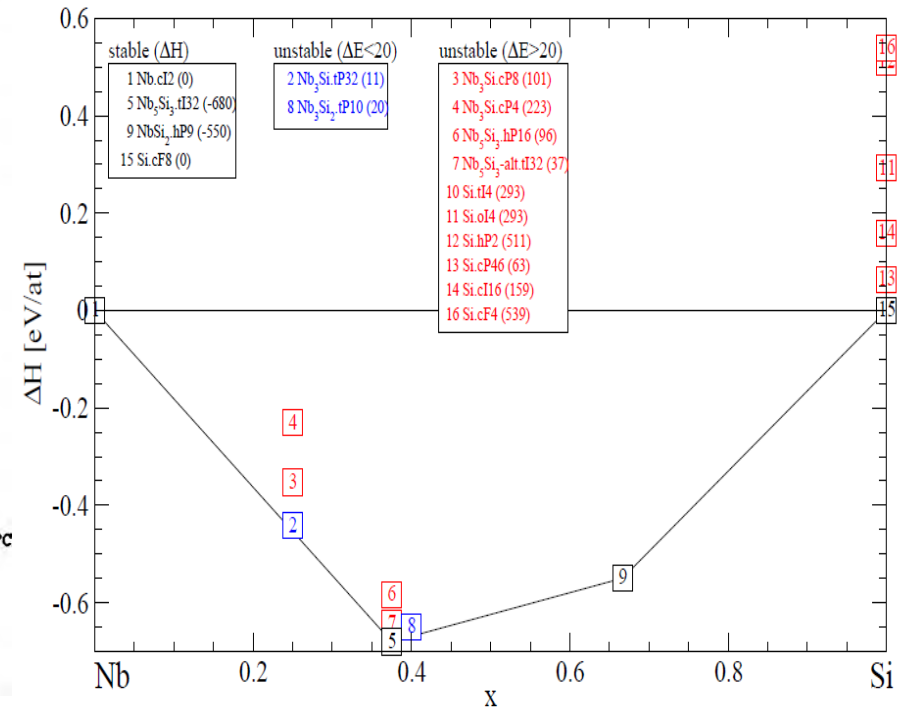
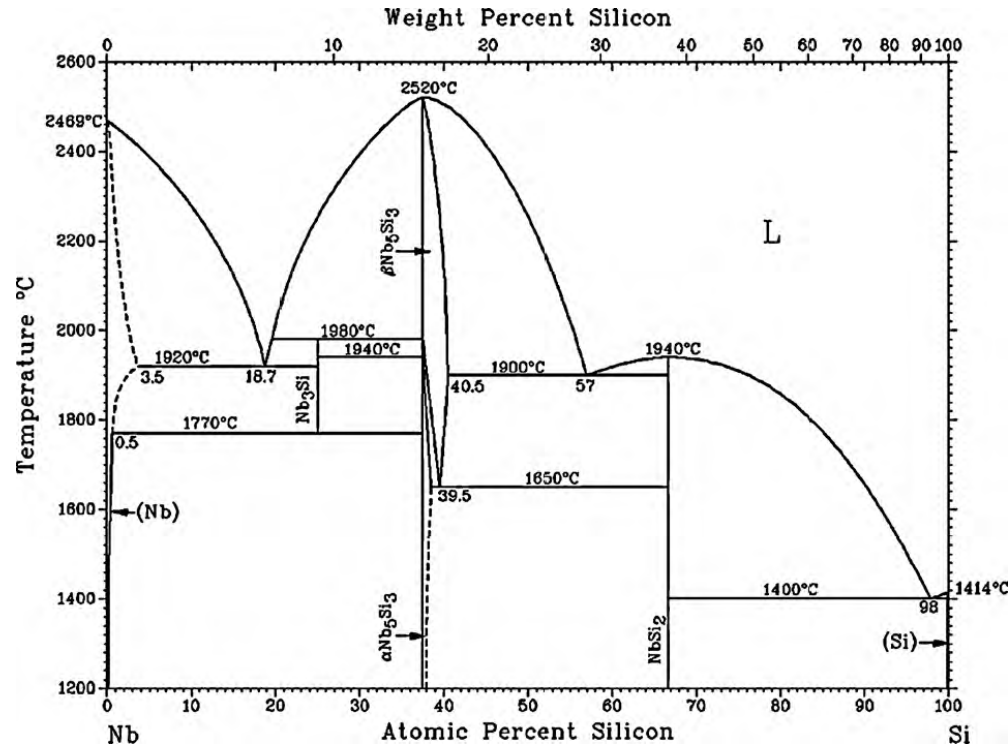


Site Occupation from Monte Carlo Simu.



Application to Nb-Si Alloys

Convex Hull Plot



Comp.	Phase	C_{11}	C_{12}	C_{13}	C_{33}	C_{44}	C_{66}	K	G
Nb	cI2								
Nb ₃ Si	cP4	111	220			72		184	21
	cP8	323	119			68		187	81
	tP32	267	175	133	284	84	95	189	78
Nb ₅ Si ₃	tI32	383	102	121	334	131	121	198	127
	tI32'	381	123	112	329	87	129	198	110
	hP16	327	153	99	359	1132	87		
Nb ₃ Si ₂	tP10	349	136	127	298	131	118	197	116
NbSi ₂	hP9	349	76	80	442	126	136	179	138

(Unit: GPa)

- ❑ Developed and tested the temperature-pressure dependent elastic constants module, equation of state $P(V,T)$ in $G(P,T)$
- ❑ Implemented the unitcell expansion method within the $G(P,T)$ package. Further testing is needed.

- ❑ Compute thermodynamic and mechanical properties of additional phases found in the Nb-Si-Cr-X alloy systems.
- ❑ Beyond quasi-harmonic approximation: (for high temperature and ambient pressure region)
 - $$d\omega_i(\{\mathbf{a}\}, T) \approx \frac{\partial \omega_i(\{\mathbf{a}\})}{\partial \varepsilon_j} d\varepsilon_j + \frac{\partial \omega_i(\{\mathbf{a}\})}{\partial \langle Q_i \rangle} \times \frac{\partial \langle Q_i \rangle}{\partial T} dT$$
- ❑ Free energy calculations for system under external field:
magnetic free energy

DOE-NETL /UCR-HBCU program

People:

Dr. Yu Shen

Mr. Michael Gray (Undergraduate)